

Self-enrichment by AGB stars in Globular Clusters: comparison between intermediate and high metallicities

P. Ventura^{*} and F. D’Antona

INAF, Osservatorio di Roma, MONTEPORZIO, I-00040, Italy

Accepted . Received ; in original form

ABSTRACT

We present theoretical evolutionary sequences of intermediate mass stars ($M=3\text{--}6.5 M_{\odot}$) with metallicity $Z=0.004$. Our goal is to test whether the self-enrichment scenario by massive Asymptotic Giant Branch stars may work for the high metallicity Globular Clusters, after previous works by the same group showed that the theoretical yields by this class of objects can reproduce the observed trends among the abundances of some elements, namely the O-Al and O-Na anticorrelations, at intermediate metallicities, i.e. $[\text{Fe}/\text{H}]=-1.3$. We find that the increase in the metallicity favours only a modest decrease of the luminosity and the temperature at the bottom of the envelope for the same core mass, and also the efficiency of the third dredge-up is scarcely altered. On the contrary, differences are found in the yields, due to the different impact that processes with the same efficiency have on the overall abundance of envelopes with different metallicities. We expect the same qualitative patterns as in the intermediate metallicity case, but the slopes of some of the relationships among the abundances of some elements are different. We compare the sodium–oxygen anticorrelation for clusters of intermediate metallicity ($Z \approx 10^{-3}$) and clusters of metallicity large as in these new models. Although the observational data are still too scarce, the models are consistent with the observed trends, provided that only stars of $M \gtrsim 5 M_{\odot}$ contribute to self-enrichment.

Key words: Stars: AGB and post-AGB; stars: abundances; globular clusters: general

1 INTRODUCTION

Spectroscopic investigations of Globular Clusters (GC) show star to star differences in their surface chemistries (Kraft 1994). These inhomogeneities trace clear abundance patterns involving all the light elements: sodium is correlated to aluminium and anticorrelated to oxygen, whereas magnesium is anticorrelated with aluminium (Carretta 2006), though in some clusters the existence of this latter relationship is still under debate (Cohen & Meléndez 2005). A common result of these analysis is the approximate constancy of the overall CNO abundances (Ivans et al. 1999).

The detection of such anomalies in scarcely evolved stars, like Turn-Off (TO) and Sub-Giant Branch (SGB) stars (Gratton et al 2001), ruled out the possibility of any in situ mechanism as a possible unique explanation (Denissenkov & Weiss 2004), and pointed in favour of a self-enrichment scenario, i.e. that the stars with the anomalous chemistry formed from the ashes of a previous stellar generation, which polluted the interstellar medium with matter which had

been processed via the CNO cycle. Ventura et al. (2001) indicated the massive Asymptotic Giant Branch (AGB) stars as likely candidates, because with appropriate hypothesis concerning convection modelling they can easily achieve Hot Bottom Burning (HBB), i.e. the bottom of their envelope becomes so hot to ignite strong nucleosynthesis, whose products, convected to the surface of the star, are ejected into the interstellar medium via the strong winds suffered by these sources (Ventura & D’Antona 2005); also, strong HBB favours high mass loss, reduces the number of thermal pulses (TP) experienced by the stars during their life, thus diminishing the number of third dredge-up (TDU) episodes, and keeping approximately constant the C+N+O mass fraction in the envelope, for a reasonably large range of initial masses. This conclusion is at odds with the results by Fenner et al. (2004), who, based on AGB models calculated with the traditional, low efficiency, mixing length theory (MLT, Vitense 1953) convective model, found that oxygen can be hardly depleted at the surface of these stars, and the CNO sum is expected to largely exceed unity.

Recently, an alternative self-enrichment scenario for GCs was proposed by Maeder & Meynet (2006), Prantzos & Charbonnel (2006), and described in details by Decressin

^{*} E-mail: ventura@oa-roma.inaf.it (PV); dantona@oa-roma.inaf.it (FD)

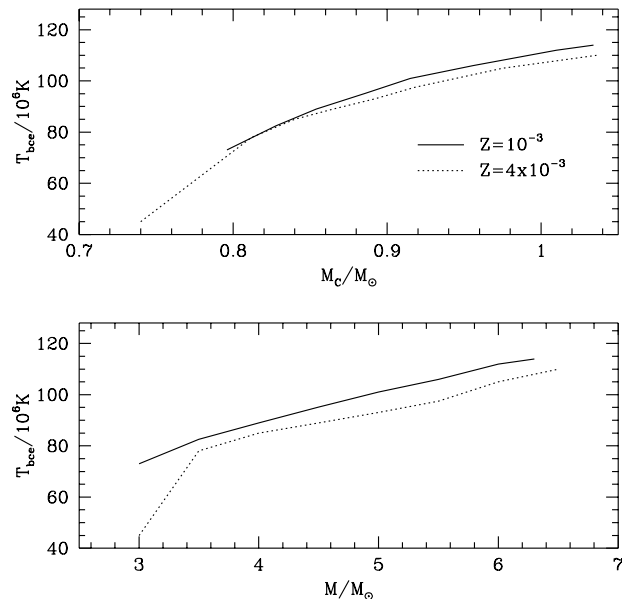


Figure 1. The variation of the temperature at the bottom of the convective envelope as a function of the core mass at the beginning of the AGB phase (Top) and of the initial mass (Bottom) of AGB models with two different metallicities. The temperatures refer to the phase of maximum luminosity during the AGB evolution.

et al. (2007): in this case the enrichment of the interstellar medium is produced by the envelopes of fast rotating massive stars. In order to choose between the AGB and the massive stars self-enrichment, it is necessary to explore in detail both models. In particular, the variation of predictions of yields with metal abundance must be examined. Ventura & D’Antona (2008, hereinafter VD08) showed that the enrichment by AGBs can work in the case of intermediate metallicity GCs, since the ejecta of their theoretical models, calculated with a metallicity $Z=0.001$, with initial masses in the range $5-6 M_{\odot}$, are in qualitative and quantitative agreement with the abundance patterns observed in scarcely evolved stars of M3, M13, M5, NGC6218, NGC6752.

The goal of the present paper is to investigate whether the self-enrichment scenario hypothesis may work also in the case of metal rich GCs, having metallicities $[\text{Fe}/\text{H}] \sim -0.7$. We present a new set of AGB models with metallicity $Z=4 \times 10^{-3}$, typical of metal rich GCs like 47Tuc and M71. We discuss the possibility of reproducing the O-Al and O-Na anticorrelations, and determine the expected slope of these relationships compared to the intermediate metallicity case.

2 THE MODELS

2.1 Physical and chemical inputs

The evolutionary sequences were calculated by means of the ATON code for stellar evolution, a full description of which is given in Ventura et al. (1998), with the last updates given in Ventura & D’Antona (2005). The physical and chemical inputs coincide with those given in VD08, with the only exception of the metallicity, for which we use $Z=4 \times 10^{-3}$ in

the present investigation. We briefly recall the main assumptions:

- Convection is modelled according to the Full Spectrum of Turbulence (FST) model by Canuto & Mazzitelli (1991)
- Mass loss is treated according to Blöcker (1995); for the free parameter entering the Reimer’s formula, we used $\eta_R = 0.02$
- Nuclear burning and mixing of chemicals are treated simultaneously, following the diffusive approach by Cloutmann & Eoell (1976); the parameter ζ giving the exponential decay of convective velocities within regions radiatively stable was set to $\zeta = 0.02$. The debate concerning a possible extra-mixing from the bottom of the convective envelope during the TDU is still open, and the uncertainties associated to this issue are such that we prefer not to include it in the present work (see Herwig 2005 for an exhaustive discussion on this topic).
- The NACRE compilation was used for all the relevant cross-sections, with the only exception of the Ne-Na proton capture rates, for which we used the formulae given by Hale et al. (2002; 2004), and the nitrogen proton capture cross section, for which we used the new rate given by Formicola et al. (2004)
- The mixture is assumed to be α -enhanced, with $[\alpha/\text{Fe}] = +0.4$ ¹. Compared to the standard solar mixture, the abundances of ^{16}O , ^{20}Ne and ^{24}Mg are increased. The individual abundances are taken from Grevesse & Sauval (1998)

2.2 The physical properties

All the models were followed from the pre-MS phase up to the almost complete consumption of the convective envelope. We find HBB in all cases, with the only exception of the $3 M_{\odot}$ model.

Fig.1 shows the comparison between the main physical properties of the present set of models and those published in VD08. The two panels show the temperature at the bottom of the envelope (T_{bce}) as a function of the initial mass of the star (bottom panel) and of the core mass (M_C) at the beginning of the AGB phase (top). The plotted temperatures refer to the phase when the maximum luminosity is reached, before the decline of $\log(L/L_{\odot})$ due to the reduction of the mass of the envelope: these quantities can be used as indicators of the degree of nucleosynthesis which we expect at the bottom of the outer convective zone.

As expected, for a given initial mass, the lower metallicity models are hotter and more luminous; yet, the $M_C - T_{bce}$ relation is approximately the same for the two set of models, thus the larger metallicity simply increases the initial mass at which a given degree of nucleosynthesis can be achieved in the outer convective envelope. The maximum T_{bce} reached in the present set of models is $T_{bce} = 107\text{MK}$, i.e. almost coincident with the maximum value found in VD08. The efficiency of the third dredge up is also similar to what was found in the lower metallicity case: the parameter² λ is $\lambda = 0.3$ dur-

¹ We use the standard notation, defining $[\text{X}/\text{Fe}] = \log(\text{X}/\text{Fe}) - \log(\text{X}/\text{Fe})_{\odot}$

² We indicate with λ the ratio between the inner penetration (in

ing the latest evolutionary phases of the $6 M_{\odot}$ model, and increases up to 0.7 for $M = 4 M_{\odot}$.

2.3 The chemical yields

Table 1 reports the average chemical content of the ejecta of the $Z = 4 \times 10^{-3}$ set of models.

We note systematic differences compared to VD08, particularly for the most massive models: aluminum is produced at a lower extent, oxygen is less depleted, and sodium is synthesized in greater quantities. Also, the CNO ratio, giving the increase of the overall CNO abundances with respect to the initial mass fractions, exceeds 2 only for the lowest masses. The carbon and nitrogen yields are also different: the ^{12}C yields are systematically lower, whereas the nitrogen production is similar in the two cases.

The aforementioned differences cannot be ascribed to the different nucleosynthesis achieved at the bottom of the convective zone, since we find similar temperatures for the same core mass, independently of Z . The main point here is that increasing the overall metallicity, hence the mass fractions of the individual species, makes harder to change the abundances of the elements in the whole envelope: this holds both in the cases of HBB and TDU. Particularly for this latter mechanism, less relevant changes are expected at higher metallicity for the same λ .

To make this point clearer, we show in the left panel of Fig.2 the variation of the abundances of oxygen (top) and aluminium (bottom) for the two sets of models; the right panel shows the behaviour of the surface sodium. We chose the mass as abscissa, to have a direct idea of the yield expected for a given element, whereas on the y-axis we put the ratio of the current over the initial abundance, thus providing an indication of the change of the individual mass fractions.

It is clear from the left panel of Fig.2 that for both O and Al the changes of the surface abundances are smaller in the $Z=0.004$ set. Oxygen is depleted at approximately the same extent as in the $Z=0.001$ case, yet the variation with respect to the starting abundance is smaller (note that this trend is opposite for the lowest masses, where oxygen is indeed produced by the TDU, and never burnt, due to the modest HBB found for $M \leq 4 M_{\odot}$). The dichotomy in the Al production is even more evident: Aluminum is produced both via HBB and also, indirectly, by the TDU, and both mechanisms, for the same temperatures and λ , have a modest effect on the surface chemistry in the $Z=0.004$ case. With respect to sodium (see the right panel of Fig.2), the question is more tricky, since the trend with mass changes during the evolution. We note a larger percentage increase in the low metallicity models at the beginning of the AGB evolution, but a stronger depletion in the following phases, when the proton capture reactions by ^{23}Na nuclei favours the sodium depletion; since this latter phase is longer than the production process, we find on the average a larger production of sodium in the $Z=0.004$ models.

mass) of the bottom of the convective envelope during the TDU and the advance of the CNO shell from the previous TP

2.4 A comparison with other AGB yields

We compare our AGB yields with those found, for the same range of masses and metallicity, with the most extended, published, computations, based on real model evolution, by Karakas & Lattanzio (2007, hereinafter KL07).

The comparison between the results is shown in Fig. 3. The three panels show, for each value of the initial mass, the CNO abundances; the quantity shown in the y-axis is actually the ratio of the average abundance compared to the initial value, in a logarithmic scale.

For the largest masses of our sample, we see two important differences between the two sets of models:

- (i) Our models destroy carbon, up to 1dex for the $6 M_{\odot}$ model, while the models by KL07 actually produce it in all cases
- (ii) Both sets of models produce nitrogen, but our models production is a factor ~ 10 smaller than KL07
- (iii) The CNO sum is very different in the two cases: it is approximately constant in our simulations (see col.10 of tab. 1), whereas it increase by a factor 10 in the KL07 models

These differences, though large, are actually not surprising, since the two sets of models have been calculated with a different treatment of convection and of mass loss. Ventura & D'Antona (2005a) showed that when convection is modelled efficiently, e.g. with the FST model used in the present investigation, HBB is favoured, the evolution is much faster, and the number of TPs and of TDU episodes experienced by the stars during the AGB phase is greatly reduced. The much larger abundances of carbon and nitrogen found in the KL07 are a mere consequence of the many TDUs experienced by their models, as a direct consequence of the much higher number of TPs determined by the MLT modelling of convection. An important difference is for example that 107 TPs are experienced by the $6 M_{\odot}$ model by KL07 (see their tab.4), whereas only 26 by our $6 M_{\odot}$ star. This difference is due in part to the large luminosity determined by the FST modelling, that favours a larger mass loss, and in part to the different prescription for mass loss used by the two groups, since the Blöcker (1995) recipe predicts a more rapid increase in mass loss with luminosity than the Vassiliadis & Wood (1993) formula used by KL07.

3 ABUNDANCE TRENDS EXPECTED IN CLUSTERS OF HIGHER METALLICITY

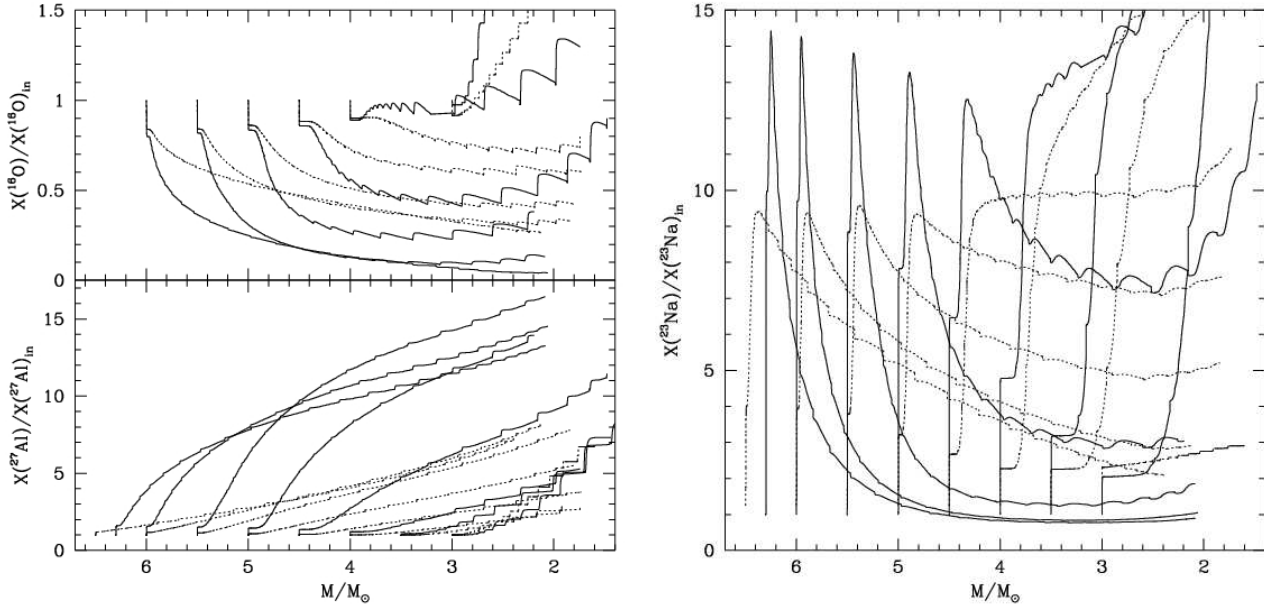
We can now compare the present results and those for smaller metallicity presented in VD08. In the hypothesis that self-enrichment in GCs is determined by the chemistry of the most massive AGBs, we can expect systematic trends with metallicity. The largest difference is that metal rich cluster should show a milder oxygen depletion, limited to ~ 0.4 dex, against the ~ 0.8 dex for the $Z=0.001$ case.

3.1 The sodium — oxygen anticorrelation

In the plane sodium vs. oxygen, the O-Na relationship at $Z \sim 0.004$ clusters is expected to have a higher slope than at $Z \sim 0.001$, as the models with $Z=0.004$ show a slightly higher enhancement of sodium, $\sim [^{23}\text{Na}/\text{Fe}] = 0.7$ and a much lower

Table 1. Chemical composition of the ejecta of intermediate mass models

M/M_{\odot}	Y	Li	$^{12}\text{C}/\text{Fe}$	$^{14}\text{N}/\text{Fe}$	$^{16}\text{O}/\text{Fe}$	$^{23}\text{Na}/\text{Fe}$	$[\text{Mg}/\text{Fe}]$	$^{27}\text{Al}/\text{Fe}$	R(CNO)
3.0	.277	1.42	1.41	0.60	0.62	0.44	0.59	0.68	4.7
3.5	.269	2.63	0.08	1.59	0.46	1.07	0.50	0.33	2.5
4.0	.281	2.20	-0.07	1.52	0.30	1.17	0.48	0.32	2.0
4.5	.298	2.00	-0.44	1.52	0.21	1.00	0.47	0.43	1.8
5.0	.313	1.98	-0.55	1.44	0.09	0.89	0.45	0.57	1.4
5.5	.328	1.93	-0.62	1.37	0.01	0.76	0.43	0.70	1.2
6.0	.329	2.02	-0.78	1.25	0.01	0.63	0.42	0.71	1.0
6.5	.330	2.06	-0.85	1.19	0.05	0.60	0.43	0.66	0.96

**Figure 2.** **Left:** The variation with the total stellar mass of the surface abundances of oxygen (Top) and aluminium (Bottom) during the AGB phase of intermediate mass models with metallicity $Z = 10^{-3}$ (solid track) and $Z = 4 \times 10^{-3}$ (dotted). For both elements, the ratio with respect to the initial values are shown. **Right:** The variation of the surface sodium abundances for the same models of the left panel.

depletion of oxygen. Note that this prediction is independent of the uncertainties related to the Ne-Na-Al proton capture cross sections, which, on the other hand, limit considerably the predictive power concerning the sodium and aluminum enhancement shown by the ejecta of AGBs (Izzard et al. 2007; VD08).

In the left side of Fig.4 we plot the sodium versus oxygen abundances in several GCs of metallicity close to $Z=0.001$ or to $Z=0.004$. Notice that the relative errors in the points location is at least ~ 0.1 dex in the abundances, and that it is not easy to judge possible additional systematic differences between abundance determination by different researchers. The connected squares represent the abundances expected in the AGB ejecta of masses from $3.5 M_{\odot}$ (upper square on the right) to $6.3 M_{\odot}$ for metallicity $Z=0.001$, from VD08. The connected big open circles represent the abundances from the present models (Table 1) from 3 to $6.5 M_{\odot}$.

The comparison clusters are M5 (open triangles, from Ivans et al. 2001) and M3 (open squares, from Sneden et al. 2004), whose trend of abundances are well reproduced, and

M13 (stars, from Sneden et al. 2004). This latter cluster possibly requires a different normalization, and also shows some very extreme oxygen abundances, below $[\text{O}/\text{Fe}]=-0.4$. The latter stars, however, are all luminous giants in all GCs so far examined (Carretta 2006) and their abundances could reflect in situ mixing, possibly due to the lower mean molecular weight barrier of giants starting with extreme helium abundances $Y > 0.35$ (D'Antona & Ventura 2007). The three clusters of high metallicity included in the data are M71 (full squares, from Sneden et al. 1994), NGC 6388 (full pentagons, from Carretta et al. 2007) and NGC 6441 (full hexagons, from Gratton et al. 2007).

The stars having high oxygen and low sodium can be interpreted as the first generation stars, born with the abundances of the pristine material from which the cluster formed. The stars having high sodium and possibly also low oxygen are the self-enriched stars. As the theoretical yields do not follow the trends defined by the stars, we must interpret the data of self-enriched stars as the result of mixing of matter having the yields of the AGBs with different rela-

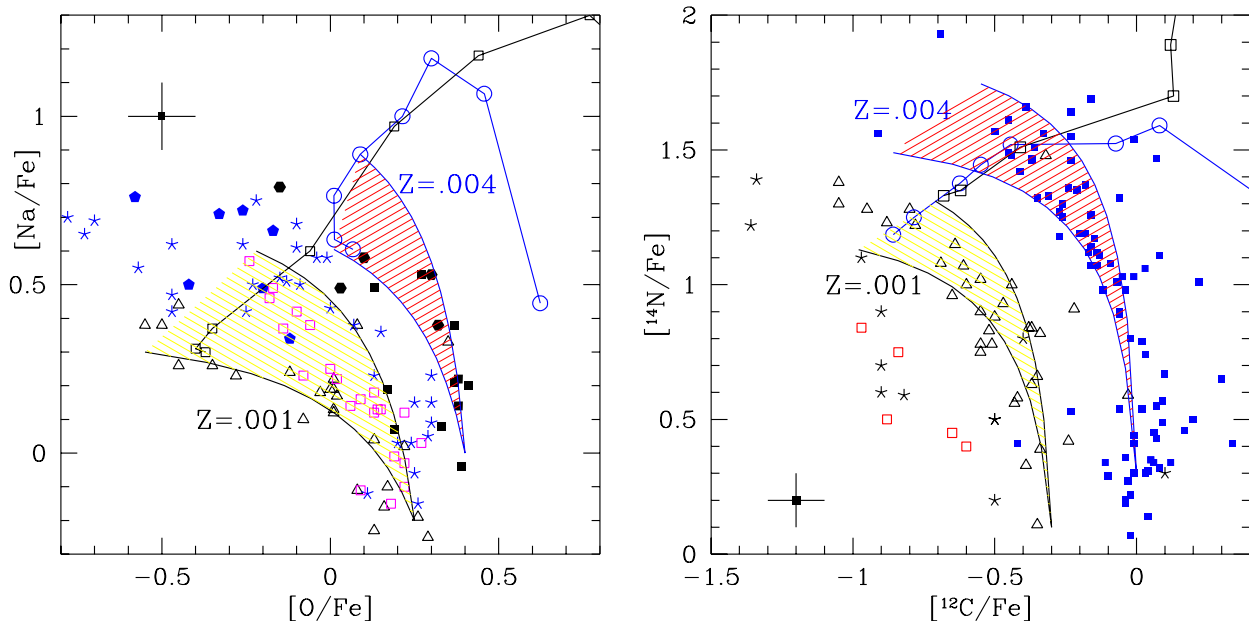


Figure 4. We show the Na–O (left) and N–C (right) anticorrelations for several GCs, in two main sets representing either metallicity close to $Z=0.004$ or to $Z=0.001$. In the left figure, the points represent abundances of sodium and oxygen from different sources. Low Z clusters: open triangles: M5 giants from Ivans et al. 2001, stars (M13) and open squares (M3) both from Sneden et al. 2004. High Z clusters: full squares: M71 from Sneden et al. 1994; full hexagons: NGC 6441 from Gratton et al. 2007; full pentagons: NGC 6388 from Carretta et al. 2007; In the right figure the full dots are the data for the main sequence in 47 Tuc (high Z), from Briley et al. 2004. Data for M5 (open triangles) are from Cohen et al. 2002, for M13 (stars) and M3 (open squares) from Cohen & Melendez 2005. A conservative error bar is also shown in the two panels. In both figures, the connected open circles are the yields from Table 1 for $Z=0.004$, while the connected open squares are the yields from VD08 for $Z=0.001$. The dashed areas represent the abundances allowed for self-enriched stars, for the two metallicities, if their chemistry results from matter lost from AGBs of masses down to $5 M_{\odot}$, diluted in different percentages with pristine matter having the chemical composition of the vertex of the shaded area (abundance of the first generation stars) chosen as representative of the most normal abundances of the stars in the two sets of clusters (see discussion in the text concerning the yield normalization).

tive amounts of pristine matter. This dilution model can be applied to the yields of all masses above $\sim 5 M_{\odot}$, for which the TDU and the lower temperatures of the HBB does not lead to too high sodium values. Among the smallest masses we consider, the total C+N+O abundance is increased due to the action of the third dredge up, but not too much. The approximate constancy of total CNO is another requirement of the observations (Ivans et al. 1999), but actually, the analysis of the CNO abundances in a few clusters by (Carretta et al. 2005) show that possibly some additional carbon from triple- α processing may be needed, consistent with our choice to include stars in which some effects of the TDU are already important.

Let us then that stars from the upper mass computed down to $5 M_{\odot}$ contribute to self-enrichment for $Z=0.001$ and $Z=0.004$. If the ejected matter and the original matter from which the GC was born are mixed in different percentages, the resulting abundances of the second generation stars will be contained in the dashed areas. Of course, part of – or also most of – the points close to the vertex of the area in fact may be stars directly formed in the first stellar generation.

In order to apply the dilution model, we have to assume an oxygen and sodium abundance for the original matter.

For M71, Fig. 4 shows that we can reasonably assume that the chemistry of the first generation stars (and of the pristine gas) is $[O/Fe] \sim 0.4$ and $[Na/Fe] \sim 0.0$. As these are the initial abundances in our models, for $Z=0.004$ we can assume that the yield abundances of the matter ejected from the AGBs are those directly given in Table 1 and in the connected circles in the figure. For the low metallicity clusters in the figure, the zero point of oxygen abundance is closer to $[O/Fe] \sim 0.25$ and $[Na/Fe] \sim -0.2$. So we have scaled down to these values the oxygen and sodium yields of AGBs, with respect to the plotted values (concerning the validity of this approach, see the discussions in Ventura & D’Antona (2005b) and VD08).

We see that the dilution model does a good job in describing the fact that the higher metallicity stars, those in M71, reach larger sodium abundances than those in the metal poor clusters, as our models predict. The data however are very scarce indeed, and require further confirmation. In addition, *all* the data points for NGC 6388 are at low oxygen – high sodium: where is the “standard” first population at high oxygen – low sodium? Also in this case, further data are needed. Although the oxygen abundances in NGC 6388 are not as extreme as in M13, we may again

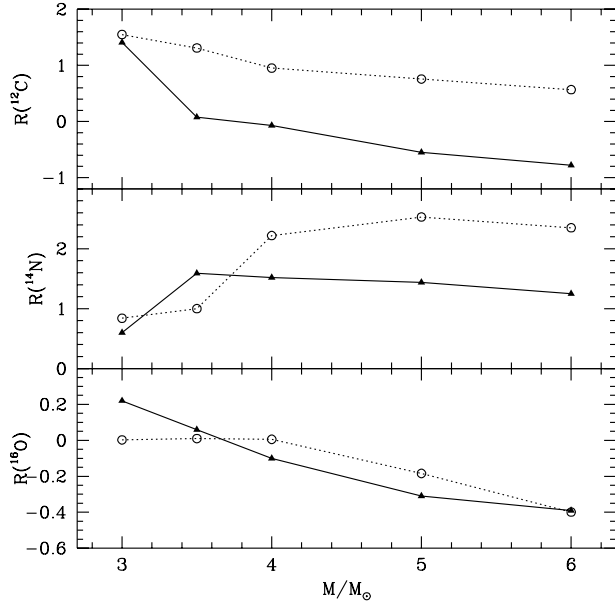


Figure 3. The average mass fractions of carbon (top panel), nitrogen (medium) and oxygen (bottom) in the ejecta of AGB models as a function of the initial mass of the star. For each element i , we show in the y-axis the quantity $\text{Log}(X_i/X_i^0)$, where X_i^0 is the initial abundance. The full triangles and the open circles indicate, respectively, the results from the present investigation and those from the KL07 models.

interpret these stars as giants suffering extra-mixing as proposed by D’Antona & Ventura (2007): this cluster, indeed, as its twin NGC 6441, has a horizontal branch morphology which implies that $\sim 20\%$ of its stars have $Y > 0.35$ (and another 40% has $0.35 < Y < 0.27$) (Caloi & D’Antona 2007; D’Antona & Caloi 2007).

In summary, Figure 4 shows that our models are in agreement with the observational data, if the range of AGB stars that contributes to self enrichment is limited down to $\sim 5 M_\odot$. However, the observations must be extended to larger samples before we can claim consistency.

3.2 Carbon and nitrogen

Another comparison between the element trends expected for different metallicities can be done on the carbon and nitrogen abundances. Unfortunately, only some of the clusters examined for the Na–O anticorrelation have also data for C and N. In the right part of Figure 4 we show the N versus C abundances for the low metallicity clusters M5 (Cohen et al. 2002), M3 and M13 (Cohen & Meléndez 2005) (same symbols as in the Na–O figure on the left). As representative of a metallicity closer to the new models, $Z=0.004$, we plot the data for stars close to the main sequence in 47 Tuc, by Briley et al. (2004); as discussed in detail by Briley et al. (2004), also M 71 has a very similar C–N behaviour. The model yields from Table 1 and from VD08, reported in Fig. 4, show that the most massive models of $Z=0.004$ (open circles) have lower ^{12}C and ^{14}N than the most massive models of $Z=0.001$ (open squares). This is easily understood, considering that the ON processing is stronger at lower metal-

licity, and therefore a larger amount of nitrogen results from the full CNO cycling. *In principle this result looks at variance with the observations*, as the 47 Tuc (high Z) data show more Nitrogen than the M5 (low Z) data. Nevertheless, the abundances derived are probably affected by a zero point uncertainty: e.g., the few data by Carretta et al. (2005)) for 47 Tuc have $[\text{C}/\text{Fe}] \sim 0.3$ dex smaller than Briley et al. (2004). Obviously, some scaling must be applied to the theoretical yields, to take into account the differences in initial abundance of the pristine matter. We already used this procedure for the sodium vs. oxygen yields, assuming that the initial values $[\text{O}/\text{Fe}]=0.4$ and $[\text{Na}/\text{Fe}]=0.0$ at $Z=0.001$ were reduced to values $[\text{O}/\text{Fe}]=0.25$ and $[\text{Na}/\text{Fe}]=-0.2$, but in the case of C and N this operation is a bit more tricky, because either the “primordial” carbon abundance of M5 is really smaller than the $[\text{C}/\text{Fe}] \sim 0$ of the models (and also of the data for 47 Tuc), or the difference may be due to a difference in absolute scale. Lower initial carbon abundances in M5 implies that less nitrogen is produced by the CN cycle, so we must also reduce the theoretical yield of Nitrogen by the same logarithmic amount. But if the difference is only a zero point problem, on the contrary, the strength of the CN band leads to derive a larger $[\text{N}/\text{Fe}]$ abundance (in fact, this could in principle give origin to an anticorrelation in the results —(Cohen et al. 2002; Briley et al. 2004)).

As the stars in 47 Tuc are easily divided in two main groups: a population where carbon and nitrogen are practically untouched, clustering at $[\text{C}/\text{Fe}] \sim 0$, $[\text{N}/\text{Fe}] \sim 0.3$, and a group of stars which define a clear C–N anticorrelation, we consider possible pollution from the range of masses between 5 and 6.5, as in the sodium vs. oxygen case, and define the dashed upper area. The data points are well contained in the region defined by the theoretical models. For $Z=0.001$ we fit the M5 data, by scaling down the carbon abundance and the total nitrogen abundance by a factor two. In this way, we are assuming that the initial C abundance of M5 is really smaller by -0.3 dex than the solar scaled value assumed in the models, and not that we are in the presence of a possible zero point uncertainty.

The comparison with M5 and 47 Tuc provides a reasonable agreement with the theoretical expectations, although the comparison remains ambiguous, as outlined above. The data for M13 and M3 are scarce and it is not clear which is the starting abundance, so no comparison with the models is attempted.

3.3 Aluminum

In the metal rich GCs, the enhancement of Aluminum should be limited to $^{27}\text{Al}/\text{Fe}=0.6$, to be compared to $^{27}\text{Al}/\text{Fe} \simeq 1$ in the $Z=0.001$ case described in VD08. Thus we expect again an O–Al anticorrelation in higher metallicity GCs, with the same trend of the O–Al anticorrelation in lower metallicity clusters, but extended to less extreme abundances of O and Al. We show in Fig. 5 the Al–O data for M13 and M3 from Sneden et al. (2004), for M71 from Ramirez & Cohen (2002), and the yields from the models of $Z=0.001$ and $Z=0.004$. We then perform the same analysis made for Na–O and N–C in Fig. 4. We assume that the abundances derive from different mixtures of matter ejected by the stars in the range $5\text{--}6.3 M_\odot$ ($Z=0.001$) or $5\text{--}6.5 M_\odot$ ($Z=0.004$) with pristine matter having abundance

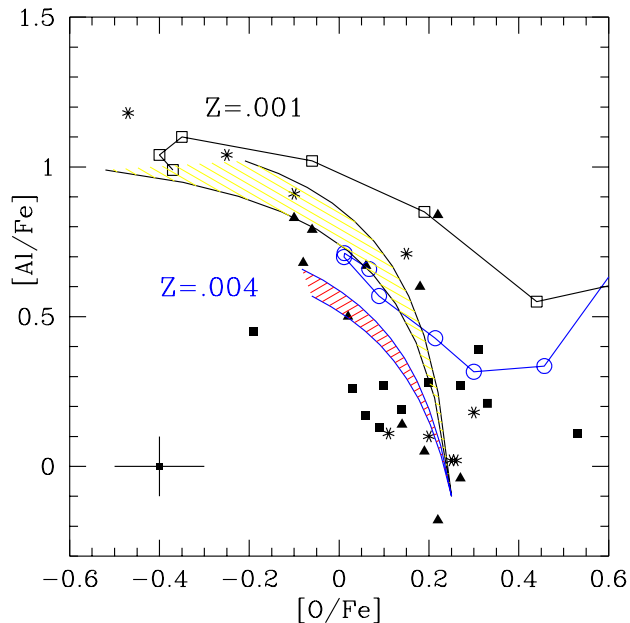


Figure 5. We show the Al-O anticorrelation for M3 (full triangles), and M13 (asterisks) from Sneden et al.(2004), and for M71 (full squares) by Ramirez & Cohen (2002). The yields for $Z=0.001$ (open squares) and for $Z=0.004$ (open circles) are also plotted. The two dashed regions represent the abundances allowed for self-enriched stars, as in Fig. 4.

$[O/Fe]=0.25$ and $[Al/Fe]=0.1$. The dashed areas show the difference between the two metallicities predictions. We also see that the M3 and M13 data are in very good agreement with the expectations for $Z=0.001$. Notice that, while the models predict that the Na-O and N-C anticorrelations should show large spread, *the Al-O anticorrelation should be much more tight* as the oxygen and aluminum yields of the range of masses allowed are very close. The data for M 71 have in fact much smaller Al variations than the low Z clusters data, but a stringent comparison would need many more data.

4 CONCLUSIONS

We present new AGB models with metallicity $Z=0.004$, to test the hypothesis of AGB self-enrichment in high metallicity GCs and compare the results with previous models having $Z=0.001$ (VD08). We find that the main physical features of the AGB evolution of the intermediate mass stars do not change by increasing the metallicity, the main effects being only a shift towards higher masses of the mass-luminosity relationship; models with the same core mass and different Z follow very similar evolution, in terms of the temperature reached at the bottom of their convective envelope.

The theoretical yields of the most massive AGB models are in agreement with the aluminum, sodium and oxygen abundances of the most anomalous stars (those showing

the strongest depletion of oxygen —and excluding the giant in which the very low O should be attributed to deep extramixing) in the few high metallicity GCs so far examined; a reasonable dilution scheme gives results consistent with the O-Na and C-N anticorrelations. Yet, other confirmation is needed, since the data currently available involve only few stars per cluster.

One robust prediction of this investigation, which is independent of all the uncertainties associated to the proton capture cross sections by Ne-Na-Al nuclei, is that with increasing metallicity we expect a higher slope of the O-Na anticorrelation, and a similar slope (though less extended) of the O-Al trend.

REFERENCES

- Blöcker, T. 1995, A&A, 297, 727
- Briley, M. M., Harbeck, D., Smith, G. H., & Grebel, E. K. 2004, AJ, 127, 1588
- Caloi, V. & D’Antona, F. 2007, A&A, 463, 949
- Canuto, V. M., & Mazzitelli, I. 1991, ApJ, 370, 295
- Carretta, E., Gratton, R. G., Lucatello, S., Bragaglia, A., & Bonifacio, P. 2005, A&A, 433, 597
- Carretta, E. 2006, AJ, 131, 1766
- Carretta, E., et al. 2007, A&A, 464, 967
- Cloutmann, L., & Eoll, J.G. 1976, ApJ, 206, 548
- Cohen, J. G., Briley, M. M., & Stetson, P. B. 2002, AJ, 123, 2525
- Cohen, J. G. & Meléndez, J. 2005, AJ, 129, 303
- D’Antona, F., & Ventura, P. 2007, MNRAS, 379, 1431
- D’Antona, F., & Caloi, V. 2007, to appear in the Proceedings of IAU Symposium 246 “Dynamical Evolution of Dense Stellar Systems”, E. Vesperini, M. Gierzs& A. Sills, eds., Cambridge University Press, astro-ph arXiv:0709.4601
- Decressin, T., Meynet, G., Charbonnel, C., Prantzos, N., Ekström, S. 2007, A&A, 464, 1029
- Denissenkov, P. A., & Weiss, A. 2004, ApJ, 603, 119
- Fenner, Y., Campbell, S., Karakas, A. I., Lattanzio, J. C., & Gibson, B. K. 2004, MNRAS, 353, 789
- Formicola, A., Imbriani, G., Costantini, H., et al. 2004, Phys. Lett. B, 591, 61
- Gratton, R. G., Bonifacio, P., Bragaglia, A., et al. 2001, A&A, 369, 87
- Gratton, R. G., Lucatello, S., Bragaglia, A., et al. 2007, A&A, 464, 953
- Grevesse, N. & Sauval, A. J. 1998, Space Science Reviews, 85, 161
- Hale, S. E., Champagne, A. E., Iliadis, C., Hansper, V. Y., Powell, D. C., & Blackmon, J. C. 2002, Phys. Rev. C, 65, 5801
- Hale, S. E., Champagne, A. E., Iliadis, C., Hansper, V. Y., Powell, D. C., & Blackmon, J. C. 2004 Phys. Rev. C, 70, 5802
- Herwig, F. 2005, ARA&A, 43, 435
- Ivans, I.I., Sneden, C., Kraft, R.P., et al., 1999, AJ, 118, 1273
- Ivans, I. I., Kraft, R. P., Sneden, C., Smith, G. H., Rich, R. M., & Shetrone, M. 2001, AJ, 122, 1438
- Izzard, R. G., Lugaro, M., Karakas, A. I., Iliadis, C., & van Raai, M. 2007, A&A, 466, 641

- Karakas, A. & Lattanzio, J. C. 2007, PASA, 24, 103
 Kraft, R. P. 1994, PASP, 106, 553
 Maeder, A., & Meynet, G. 2006, A&A, 448, L37
 Prantzos, N., & Charbonnel, C. 2006, A&A, 458, 135
 Ramírez, S. V., & Cohen, J. G. 2002, AJ, 123, 3277
 Sneden, C., Kraft, R. P., Langer, G. E., Prosser, C. F., & Shetrone, M. D. 1994, AJ, 107, 1773
 Sneden, C., Kraft, R. P., Guhathakurta, P., Peterson, R. C., & Fulbright, J. P. 2004, AJ, 127, 2162
 Vassiliadis, E., & Wood, P. R. 1993, ApJ, 413, 641
 Ventura, P., D'Antona, F., Mazzitelli, I., & Gratton, R. 2001, ApJ Letters, 550, L65
 Ventura, P., & D'Antona, F. 2005a, A&A, 431, 279
 Ventura, P., & D'Antona, F. 2005b, A&A, 439, 1075
 Ventura, P., & D'Antona, F. 2008, A&A, in press
 Ventura, P., Zeppieri, A., D'Antona, F., & Mazzitelli, I. 1998, A&A, 334, 953
 Vitense, E. 1953, Zs.Ap., 32, 135